

Design of a small-scale organic Rankine cycle engine used in a solar power plant

E. Georges*, S. Declaye, O. Dumont, S. Quoilin and V. Lemort

Thermodynamics Laboratory, University of Liege, Chemin des chevreuils 7, 4000 Liege, Belgium

Abstract

Under the economic and political pressure due to the depletion of fossil fuels and global warming concerns, it is necessary to develop more sustainable techniques to provide electrical power. In this context, the present study aims at designing, building and testing a small-scale organic Rankine cycle (ORC) solar power plant (~ 3 kWe) in order to define and optimize control strategies that could be applied to larger systems. This paper presents a first step of the design of the solar power plant and focuses more specifically on the ORC engine. This design is defined on the basis of simulation models of the ORC engine and takes into account some technical limitations such as the allowed operating ranges and the technical maturity of the components. The final configuration includes a diaphragm pump, two plate heat exchangers for the regenerator and the evaporator, an air-cooled condenser, two hermetic scroll expanders in series and R245fa as the working fluid. Simulations indicate that an efficiency close to 12% for the ORC engine can be reached for evaporating and condensing temperatures of 140 and 35°C, respectively.

Keywords: Organic Rankine cycle; scroll expander; small-scale solar power plant

*Corresponding author:
emeline.georges@ulg.ac.be

Received 18 January 2013; revised 1 April 2013; accepted 7 April 2013

1 INTRODUCTION

Over the last century, economic development in many areas has entailed tremendous growth in energy consumption through the intensification of the industrial sector, increase in domestic consumption and growth of the automobile industry. Thus far, this increase in energy demand has been met mainly by the massive use of fossil fuels, leading to the depletion of their resources and to atmospheric pollution.

Recent concerns pertaining to energy supply security and climate change mitigation have encouraged the development of alternative energy sources and of heat recovery technologies. Over the last decade, organic Rankine cycles (ORCs) have widely been studied to harness low-grade heat sources that provide temperatures ranging between 80 and 400°C.

An ORC includes the same components as a traditional Rankine cycle, namely a pump, an evaporator, a turbine (or expander) and a condenser. The major difference comes from the choice of working fluid: water is replaced by an organic component.

One of the earliest studies related to this technology was carried out by Davidson [1] in 1977 with the design and analysis of a 1 kW prototype for solar applications. The fluid selection was discussed a few years later by Badr *et al.* [2]. Commercial applications started in the late 1970s and interest in this

technology has risen significantly over the last decade. Currently, there are more than 200 installed and operating ORC plants around the world, for an installed power in excess of 1.5 GW [3]. Biomass applications are the most widespread with a scale of about 1 MWe per unit. In terms of installed power per unit, geothermal applications can reach more than 10 MWe and account for most of the installed power. Other applications such as solar power plants, waste-heat recovery or bottoming cycle applications have so far been less widespread. Therefore, an additional study of solar ORCs seemed to be a useful contribution to the field.

Small-scale solar ORCs of a few kilowatts have also been studied in the 1970s by Monahan [4] and in the 1980s by Probert *et al.* [5], with a focus on the engine and reported efficiencies below 10%. Different technologies of concentrating collectors can be used for ORC solar power plants, such as solar towers, parabolic troughs, Fresnel linear collectors and solar dishes. More recently, Kane *et al.* [6] studied a cascade ORC coupled to linear Fresnel collectors with R123 and R134a as working fluids and obtained an overall efficiency of 7.74%. Flat plate collectors and evacuated tubes were used by Wang *et al.* [7]. Overall efficiencies of 4.3 and 3.2% were obtained, respectively. BouLawz Ksayer [8] conducted a study over a solar ORC for electricity and domestic hot water production for an average French dwelling. The selected working fluid was R245fa. During peak solar hours, an efficiency of 14.35% was predicted for the

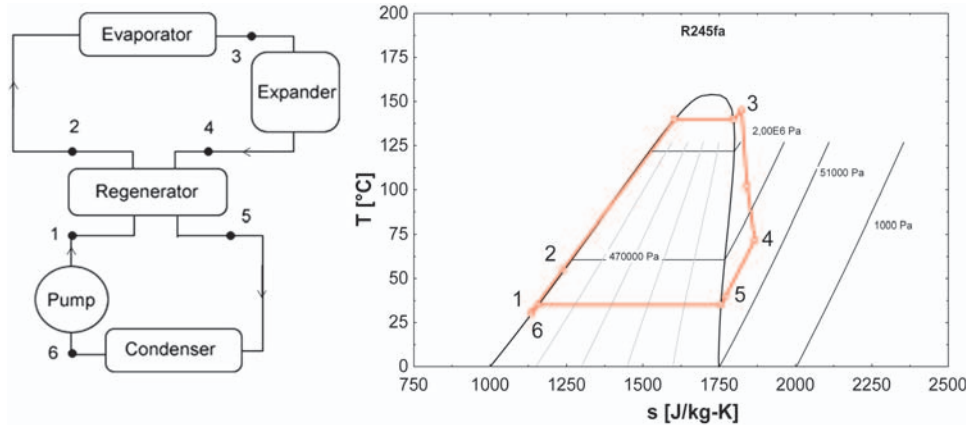


Figure 1. Basic components and T-s diagram of an ORC.

ORC part. The analysis, optimization [9] and design recommendations [10] of the low-temperature regenerative solar ORC were presented by Delgado-Torres and García-Rodríguez for water desalination in the power range of 50–500 kW. Two models of flat plate collectors, a compound parabolic collector and an evacuated tube flat plate collector, were considered, respectively, with four different fluids: isobutane, isopentane, R245fa and R245ca. A best overall efficiency of 8.51% was reached with isopentane with the evacuated tube flat plate collector.

A thermodynamic analysis and optimization of solar-driven regenerative ORC was presented by Wang *et al.* [11]. The fluid selection showed R245fa and R123 as the best candidates.

Though medium-scale solar ORCs are already available commercially, work still remains to be done for systems of a few kilowatts. For example, a small-scale low temperature (<200°C) ORC coupled to 75 m² of parabolic trough collectors has been installed in Lesotho in 2007 by the non-profit organization STG International [12, 13] for a net power output of 3 kWe. Another prototype of 5 kWe was constructed in 2009 within the frame of the project POWERSOL [14] in Almeria. The fluid used is SES36 and the announced theoretical overall and ORC efficiency are 7 and 14%, respectively, although these numbers have not been confirmed by experimental data yet.

An important component of an ORC is the expansion device. Positive displacement machines are well suited for these small-scale applications and, in particular, the use of scroll expanders technology [15]. Oralli *et al.* [16] described the conversion of a commercial scroll compressor into a scroll expander. Modeling of scroll compressors has been carried out by Bell [17]. Experimental studies of an automotive scroll expander integrated into an ORC working with R245fa and R134a have been done by Woodland [18]. In the present study, a scroll expander was also used.

2 DESCRIPTION OF THE CYCLE

The cycle presented in this paper is a regenerative ORC (Figure 1). The liquid fluid is pressurized by a pump and

Table 1. Main assumptions of the working fluid selection model.

Evaporating temperature	Condensing temperature	Net power	Expander isentropic efficiency	Pump isentropic efficiency
140°C	35°C	3 kW	70%	70%
Regenerator efficiency	Superheat	Subcooling	Evaporator pinch point	Oil maximum temperature
80%	5K	5K	5K	180°C

vaporized to a superheated state by means of a heat input. The vapor is then expanded in a turbine connected to a generator. Finally, the vapor is condensed and heat is released into the environment. A regenerator is included to use the residual high-temperature vapor refrigerant exiting the expander to preheat the liquid refrigerant after the pump. The evaporator is fed with hot oil from solar concentrator. The use of an oil loop between the solar collector and the evaporator was chosen for three main reasons: to avoid mechanical constraints due to the direct evaporation of the refrigerant in the solar collector, to diminish the charge of the refrigerant and to facilitate a possible future coupling with a thermal storage system. The cooling of the condenser is ensured by ambient air.

3 SIZING AND SELECTION OF ALL MAJOR COMPONENTS

3.1 Preselection of the working fluid

A first model of the cycle was built under EES solver [19] to select the most appropriate working fluid. This model is based on the assumptions given in Table 1.

It should be noted that pressure drops over the heat exchanger are neglected.

Six working fluids (R123, R245fa, SES36 (Solkatherm[®] SES36—azeotropic mixture of Solkane 365mfc and a perfluoropolyether), pentane, HFE7000 (3M[™] Novec[™] Engineered

Table 2. Fluid comparison results.

	R123	R245fa	Pentane	Ethanol	HFE7000	SES36
Condensing pressure (bar)	1.3	2.1	0.98	0.14	1	0.99
Evaporating pressure (bar)	17.6	28.1	13.3	7.6	15.7	14.6
Pressure ratio	13.47	13.34	13.52	55	15.66	14.77
Mass flow rate (g/s)	64.9	64.3	29.0	12	80.7	69.4
Cycle thermal efficiency	0.15	0.139	0.155	0.154	0.147	0.158
Second law efficiency	0.59	0.55	0.61	0.61	0.58	0.62
Turbine inlet volumetric flow rate (l/s)	0.59	0.35	0.78	1.1	0.57	0.61
Turbine outlet volumetric flow rate (l/s)	9.1	6.2	12.1	47.6	12.1	11.41

Table 3. Fluid properties, safety and environmental impact.

Fluid	T_{crit} (°C)	Vapor saturation curve	ODP	GWP (100 years, CO ₂ = 1)	Safety*
R123 [26]	184	Isentropic	0.012	53	B1
R245fa [26]	154	Isentropic—dry	~0	950	B1
SES36	177.5	Dry	0	n.a.	n.a.
Pentane [26]	196	Dry	~0	11	A3
HFE7000 [27]	164.6	Dry	~0	370	A1
Ethanol [28]	240.8	Wet	0	<25	Inflammable

*ASHRAE classification: A, lower toxicity; B, higher toxicity.

1, no flame propagation; 2, lower flammability; 3, higher flammability.

Fluid HFE-7000) and ethanol) are compared using the model. The results are presented in Table 2. The criteria for the selection of a proper working fluid for a given ORC application are numerous [20–22]. They are mainly technical and economic but some arguments related to safety or environmental impacts have to be considered as well. In this study, six technical and economic criteria are used:

- Acceptable pressure level in the condenser: very low condensing pressure leads to low density and then high volumetric flow rate in both the condenser and the regenerator. Since pressure drops are an increasing function of fluid speed, larger (i.e. more expensive) components would have to be selected.
- Evaporating pressure lower than 30 bar to ensure compatibility with the selected expander technology (Section 3.2).
- Low pressure ratio over the expander to allow it to work in its high-efficiency region. This is further explained in Section 3.2.
- Low mass flow rate in order to limit the size of the pump.
- High cycle efficiency.
- Low expander volumetric flow rate to limit the size of the turbine.

Table 3 lists the characteristics of the different fluids in terms of properties, safety and environmental concerns. ‘Dry’ fluids (i.e. with a positive slope for their vapor saturation curves) remain in the superheated vapor region during the expansion process, which avoids the presence of a two-phase flow in the expansion device and allows the use of a regenerator. The environmental impact is estimated through the ozone depletion potential (ODP) and the global warming potential (GWP). The fluids

safety properties are stated from the ASHRAE safety classification of refrigerants.

SES36 shows the highest cycle efficiency. Ethanol is rejected since it combines the lowest condensing pressure, the highest pressure ratio and the highest expander volumetric flow rate, even though it has the smallest mass flow rate. HFE7000 is also eliminated since it shows results very similar to those for SES36 but a lower efficiency. The only advantage of pentane is the low mass flow rate, which is not enough to justify the use of a flammable fluid. R123 is also eliminated since it has a non-null ODP and will be phased out in 2030. Among the two remaining candidates, both R245fa and SES36 are considered for a more detailed comparison using advanced models. These fluids are characterized by a ‘dry’ vapor saturation curve which prevents the presence of droplets during the expansion process.

3.2 Selection of the expander

Some of the authors [23] previously presented a methodology to compare several types of expansion machines for Rankine cycles. This methodology accounted for the limitations of each expansion machine technology and several applications were investigated. According to Figure 2, for low-temperature solar applications below 10 kWe, the scroll is the most suitable machine.

Moreover, the scroll expander technology shows the following advantages:

- The widespread use of scroll machines as compressor in refrigeration applications makes them available at low cost.
- The conversion of a refrigeration compressor into an expander requires only a few modifications.

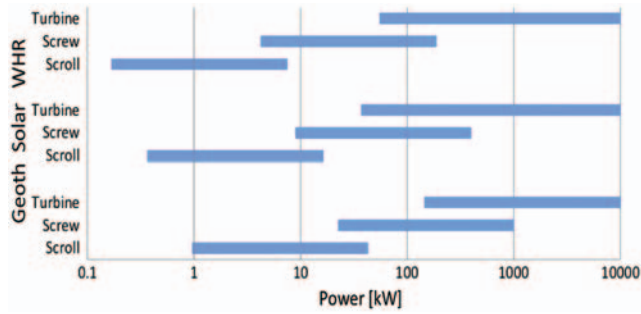


Figure 2. Comparison of expansion machines [23].

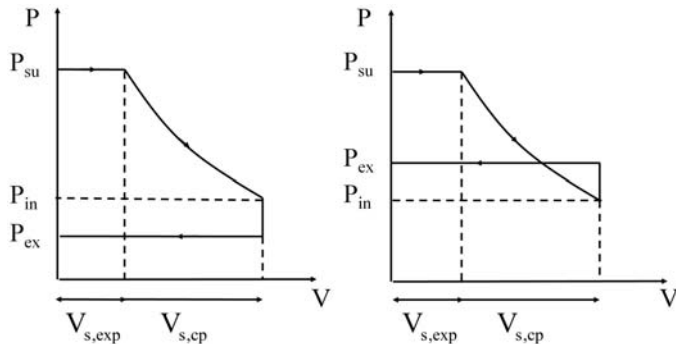


Figure 3. Losses by under-expansion (left) and over-expansion (right) [15].

- The reduced number of moving parts makes them reliable.
- Scroll machines are available at low capacities (down to a few hundred Watts).
- They can handle the presence of a liquid phase in the flow.

A significant limitation of positive displacement expanders is linked to the losses caused by the fixed built-in volumetric ratio: if the external volume ratio imposed between the inlet and the outlet of the expander is greater than the built-in volume ratio, the flow undergoes an irreversible expansion to reach the final outlet pressure. This results in under-expansion losses (Figure 3, left). On the contrary, if the external volume ratio is smaller than the internal one, some fluid flows from the discharge line into the expansion chamber causing irreversible compression (over-expansion losses (Figure 3, right)). Scroll expanders exhibit built-in volume ratios typically between 3 and 4.

Figure 4 shows a typical performance curve of scroll expander [24]. Isentropic efficiency exhibits a maximum at a pressure ratio around 4. At a low pressure ratio, the efficiency sharply decreases, whereas this decrease is more progressive at high pressure ratios.

According to the results shown in Table 2, the nominal pressure ratio of the cycle is around 15, corresponding to a nonoptimal expander efficiency if a single-stage is used. The option of using two expanders in series is therefore investigated. In this case, the total pressure ratio is split over both expanders, allowing them to operate closer to their nominal point.

Four configurations are then compared:

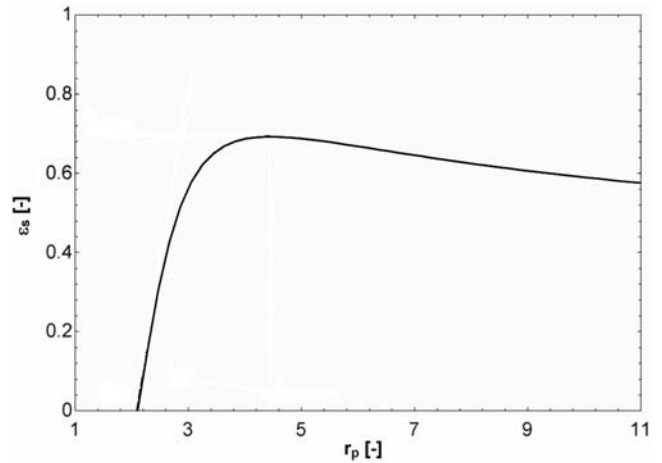


Figure 4. Scroll expander isentropic efficiency curve as a function of the pressure ratio across the expander [24].

- R245fa and one expander
- R245fa and two expanders in series
- SES36 and one expander
- SES36 and two expanders in series

The numerical model is based on the same assumptions as previously (Table 1), except for the expander model and the evaporating temperature. The expander isentropic efficiency is no longer set to a constant value, but is calculated using the semi-empirical model proposed by Lemort *et al.* [15]. In this model, the expansion process is divided into two steps: an adiabatic and reversible step followed by an adiabatic expansion at constant machine volume. In the first step, the fluid is expanded to a pressure adapted to the internal volume ratio of the expander. Then, the discharge chamber enters in contact with the discharge line. This model also takes into account the main irreversibilities occurring during the expansion process, such as inlet pressure drops, heat transfers and frictions. The evaporating temperature is set to the value that maximizes the cycle thermal efficiency but is limited to 140°C to comply with the maximum inlet temperature inherent to refrigeration scroll machines. In the case of two-stage expansion, the intermediate pressure is optimized to maximize the cycle thermal efficiency.

The main results are shown in Table 4. The cycle efficiency is defined as the ratio of the net electrical power to the heat transfer rate at the evaporator. The net electrical power is the difference between the electrical power produced by the expanders and the pump and fan electrical consumptions.

$$\eta_{\text{cycle}} = \frac{(\dot{W}_{\text{exp}} - \dot{W}_{\text{pump}} - \dot{W}_{\text{fan}})|_{\text{elec}}}{\dot{Q}_{\text{ev}}} \quad (1)$$

For both fluids, the configurations with two expanders lead to a significant improvement in the cycle thermal efficiency: an increase of 38% is stated for R245fa and of 50% for SES36. This configuration allows both expanders to work at a higher

Table 4. Comparison of expander/fluid configurations.

	R245fa		SES36	
	1 exp	2 exp	1 exp	2 exp
HP expander swept volume (cm ³)	39.92	11.42	64.27	22.77
LP expander swept volume (cm ³)		48.04		84.42
HP expander isentropic efficiency	0.59	0.69	0.521	0.699
LP expander isentropic efficiency		0.69		0.66
Pump consumption (kW)	0.2	0.29	0.166	0.185
Net power (kW)	2.8	2.71	2.83	2.81
Boiler thermal power (kW)	34	23.8	32.1	21.3
Regenerator thermal power (kW)	4.69	3.3	9.5	7.6
Condenser thermal power (kW)	30.8	20.5	28.8	17.8
Mass flow rate (kg/s)	0.159	0.105	0.203	0.129
Cycle thermal efficiency	8.2	11.36	8.83	13.21
Evaporating temperature (°C)	105.1	140	114.5	140
Evaporating pressure (bar)	14.2	28.1	8.7	14.6
Condensing temperature (°C)	35	35	35	35
Condensing pressure (bar)	2.1	2.1	0.99	0.99

isentropic efficiency than in the single-stage configuration. In the case of R245fa, both expanders show an isentropic efficiency of 0.69 and thus work close to the optimal condition set to a maximum value of 0.7 in the model. For SES36, the isentropic efficiency of the high-pressure expander is of 0.699, whereas it is slightly smaller (0.66) for the low-pressure expander.

The two-stage expansion configurations also lead to additional costs. However, these extra costs are limited since the high-pressure expander is fairly small in both cases (11.42 cm³ for R245fa and 22.77 cm³ for SES36). Moreover, the increase in cycle efficiency leads to a reduced required evaporator power for the same electrical output power. The required solar field area is, therefore, reduced by 30% for R245fa and 33% for SES36. The extra investment on expansion machines can thus be compensated for by the reduction of the solar field costs. Finally, size of the condenser is also considerably reduced in the two-stage configuration.

The cycle efficiency is higher with SES36 in both single- and two-stage expansion configurations. The evaporating pressure is also significantly smaller than with R245fa, which is an advantage in terms of safety. It is also noteworthy that the condensing power is 5–10% lower with SES36, which is not negligible in case of air cooling. However, the cycle efficiency in the two-stage expansion case with SES36 is only 16% higher than for the same configuration with R245fa, whereas the required expander swept volumes are almost doubled. Furthermore, the mass flow rate of refrigerant is significantly higher in the case of SES36 for both configurations. This requires the use of larger pumps, although the power consumption is reduced.

For the four cases under consideration, the use of the regenerator is beneficial. The power exchanged in the regenerator reaches around 15% of the evaporating power for both configurations with R245fa. With SES36, 30 and 35% of the evaporating power are obtained for the single-stage and two-stage configurations, respectively.

Table 5. Expander characteristics.

	HP expander	LP expander
Swept volume in compressor mode	46.1 cm ³	167.3 cm ³
Swept volume in expander mode	13.17 cm ³	47.8 cm ³
Synchronous speed	3000 rpm	
Maximum inlet pressure	29.5 bar	
Maximum inlet temperature	150°C	

Table 6. Main requirements of the pump.

	R245fa
Fluid	R245fa
Density	1325 kg/m ³
Flow rate	284.4 l/h
Inlet pressure	2.1 bar
Outlet pressure	28.15 bar
Viscosity	0.38 mPa s

Though SES36 shows interesting properties, the final configuration selected is R245fa with two expanders. The main reason of this choice is the significantly higher size required for both expanders for the two-stage configuration with SES36 compared with R245fa. As mentioned in Section 1, this fluid had also been selected in previous studies. However, it should be noted that because of its GWP of 1000, it will most likely be phased out in the coming years. Fluids with equivalent thermodynamic properties that present much lower GWPs, such as HCFO-1233zd(E) (GWP <5 and null ODP), are currently under study.

Since no scroll expanders are available on the market at competitive cost, two hermetic refrigeration scroll compressors are converted into expanders. The main required modifications are the removal of check valves and the addition of a spring to deactivate the unloading system of the compressor. A comprehensive description of the modifications is proposed in [12].

Given the swept volume of the expanders $V_{s,exp}$ (see Table 5), the compressor swept volume $V_{s,cp}$ is calculated by

$$V_{s,cp} = V_{s,exp} r_{v,cp}, \quad (2)$$

where $r_{v,cp}$ is the built-in volumetric ratio of the compressor, which is equal to 3.5. The main characteristics of both expanders are given in Table 5. Both maximum inlet pressure and temperature are given in the expander mode.

3.3 Selection of the pump

The pump of an ORC has to meet some requirements:

- High isentropic efficiency: the ratio of pump consumption to expander production (back work ratio) is higher for organic fluids than for water [12]. Therefore, in ORC systems, a low pump efficiency has a dramatic impact on the net power and the cycle efficiency.
- Hermetically sealed: since R245fa has a non-negligible environmental impact (GWP around 1000), the pump, as well as all the components of the cycle, have to be perfectly tight.

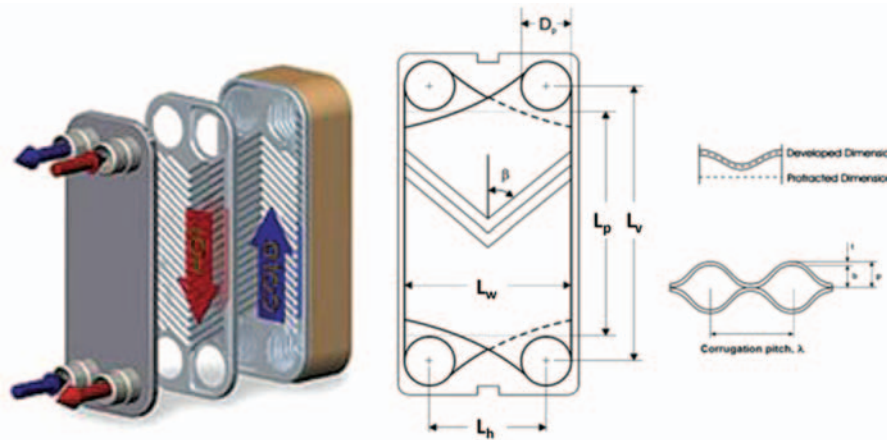


Figure 5. Braze plate heat exchanger—construction (left) [26] and parameters (right) [25].

Table 7. Main characteristics of the pump.

Flow rate	6.2 l/min
Consumption	0.41 kW
Nominal speed	1000 rpm
Max. outlet pressure	70 bar
Efficiency	70%

- Low net positive suction height to avoid cavitation issues.
- Fluid compatibility.

Pressure and flow rate requirements are given in Table 6.

Volumetric pumps are the most adapted to these working conditions (low flow rate and high pressure difference). Among the large number of volumetric pump types (gear, piston, vane, diaphragm etc.), a multidiaphragm pump is selected. The main advantage of this type of pump is the absence of contact between the fluid and pump moving parts. External leakages are, therefore, totally avoided. The main characteristics of the pump according to manufacturer data are shown in Table 7.

3.4 Selection of the heat exchangers

Both the evaporator and the regenerator are brazed plate heat exchangers (Figure 5, left). The four suction ports on each plate are used by pairs to provide access to the flows through alternated channels and in counter-current flows.

The plate is chevron type. The different parameters can be seen on the schematic in Figure 5 (right). The chevron angle, β , determines the corrugation pattern and is, therefore, related to the pressure drops and heat transfer characteristics of the plate.

The main advantages of this type of heat exchanger are [25]: the minimal risk of internal leakage, compact design, efficient heat transfers, control over pressure drops and ease of maintenance.

The main characteristics of the evaporator and regenerator are given in Table 8.

For the condenser, since no water cooling is available on the power plant site, air cooling was selected. A direct air condensation of the working fluid is chosen to avoid the use of an

Table 8. Evaporator and regenerator characteristics.

	Regenerator	Evaporator
Fluid (hot/cold)	R245fa/R245fa	Thermal Oil/R245fa
Cold side temperature (in/out) (°C)	31.6/55	55/140
Hot side temperature (in/out) (°C)	71.7/39.3	175/100
Flow rate (hot/cold) (kg/s)	0.105 / 0.105	0.146/0.105
Thermal power (kW)	3.3	23.8
Number of plates	42	100
Width/height/depth (mm)	113/313/105	191/618/230

Table 9. Main characteristics of the condenser.

Cooling capacity	20.7 kW
Fan nominal speed	700 rpm
Fan consumption	0.25 kW
Air flow rate	1.62 m ³ /s

additional heat exchanger and a rise of the condensing pressure in the case of a closed water loop solution. The maximum condenser thermal power is 20.5 kW. In order to limit the electrical consumption of condenser fans at part load, variable speed fans are selected. The main characteristics of the condenser are shown Table 9.

3.5 Final configuration

The final configuration with all measurement devices is shown in Figure 6.

4 SYSTEM COST

The components selected for this work are produced in large series and are widely used for applications such as heat pumps and vapor compression cycles. Figure 7 shows the contribution of each component to the total cost (14321€) for the ORC module only. Condenser, LP expander and evaporator account for 61% of the total cost. The pump represents 16% on its own. The small HP expander cost is only 33% of the LP expander.

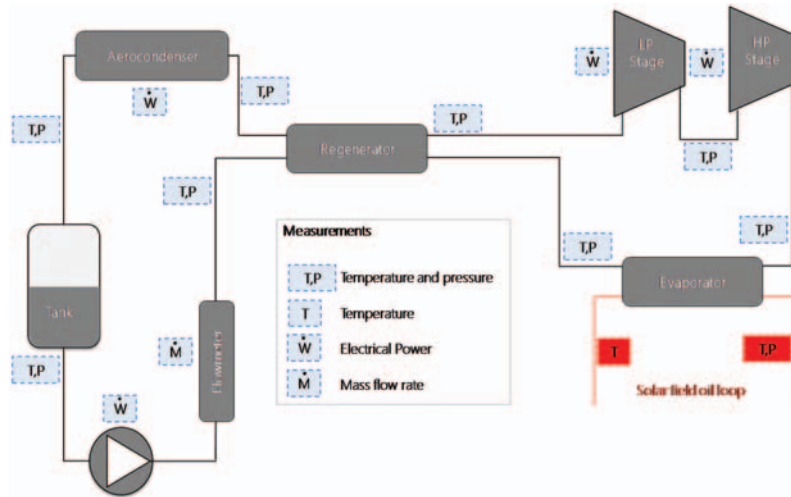


Figure 6. Final configuration.

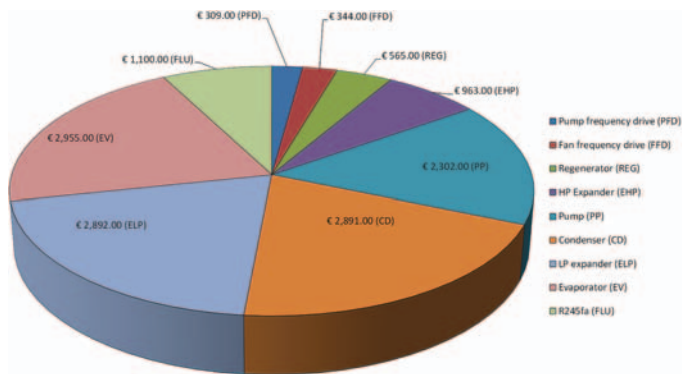


Figure 7. System cost.

That confirms that choosing R245fa instead of SES36 to reduce expander size, and therefore cost, has a great impact on the total system cost. The regenerator cost accounts for only 4% of the total component cost but increases the cycle efficiency by 10%. Frequency drives for both the pump and the expander account for 5% of the total and allow reduction of the auxiliary consumption at part load. The R245fa charge is around 22 kg and the specific cost is 50€/kg. It, therefore, accounts for 8% of the total system cost. It should be noted that these costs correspond to prototyping cost. It is likely that a larger production of such units would dramatically reduce these costs.

The influence of the working fluid on the system cost has been outlined by some of the authors in [22] and should be further explored.

5 CONCLUSIONS

The design of a solar power plant of a few electrical kilowatts based on ORC was described. The main selection criteria for each component were detailed. The final design involves two scroll expanders in series, a multidiaphragm pump and an air

condenser. The fluid selected was R245fa. Using very realistic models validated on experimental data, it has been shown that a cycle thermal efficiency higher than 11% can be achieved. This efficiency could obviously be increased by using higher temperature collectors and evaporator, but this would forbid the use of off-the-shelf widely available heating ventilation air-conditioning components such as scroll expanders, and would significantly increase the costs.

This study allowed establishing the design of the solar ORC unit. It will be followed by an experimental phase comprising the following steps:

- Testing of the solar plant using an alternative heat source for a wide range of conditions.
- The validation of semi-empirical models of each component.
- The development of appropriate control strategies.

REFERENCES

- [1] Davidson T. Design and analysis of a 1 kW Rankine power cycle employing a multi-vane expander for use with a low temperature solar collector. Massachusetts Institute of Technology, 1977.
- [2] Badr O, O'Callaghan PW, Hussien M, *et al.* Multi-vane expanders as prime movers for low grade energy Organic Rankine Cycle engines. *Applied Energy* 1984;16:129–46.
- [3] Enertime. Le Cycle Organique de Rankine et ses applications. <http://www.cycle-organique-rankine.com/technologie.php>.
- [4] Monahan J. Development of a 1-kW, Organic Rankine Cycle Power Plant for remote applications. In *Presented at the Intersociety Energy Conversion Engineering Conference*, New York, 1976.
- [5] Probert SD, Hussein M, O'Callaghan PW, *et al.* Design optimisation of a solar-energy harnessing system for stimulating an irrigation pump. *Applied Energy* 1983;15:299–321.
- [6] Kane M, Larrain D, Favrat D, *et al.* Small hybrid solar power system. *Energy* 2003;28:1427–43.

- [7] Wang XD, Zhao L, Wang JL, *et al.* Performance evaluation of a low-temperature solar Rankine cycle system utilizing R245fa. *Solar Energy* 2010;84:353–64.
- [8] BouLawz Ksayer E. Design of an ORC system operating with solar heat and producing sanitary hot water. *Energy Procedia* 2011;6:389–95.
- [9] Delgado-Torres AM, García-Rodríguez L. Analysis and optimization of the low-temperature solar organic Rankine cycle (ORC). *Energy Conversion and Management* 2010;51:2846–56.
- [10] Delgado-Torres AM, García-Rodríguez L. Design recommendations for solar organic Rankine cycle (ORC) – powered reverse osmosis (RO) desalination. *Renewable and Sustainable Energy Reviews* 2012;16:44–53.
- [11] Wang M, Wang J, Zhao Y, *et al.* Thermodynamic analysis and optimization of a solar-driven regenerative organic Rankine cycle (ORC) based on flat-plate solar collectors. *Applied Thermal Engineering* 2013;50:816–25.
- [12] Quoilin S. Sustainable energy conversion through the use of organic rankine cycles for waste heat recovery and solar applications. *Ph.D. Dissertation*. University of Liège, 2011.
- [13] Quoilin S, Orosz M, Lemort V. Modeling and experimental investigation of an Organic Rankine Cycle using scroll expander for small scale solar applications. In *Proceedings of the Eurosun Conference*, Lisbon, 2008.
- [14] Blanco Galvez J. POWERSOL Project, Mechanical power generation based on solar Thermodynamic Engines. CIEMAT-Plataforma Solar de Almería, 2009.
- [15] Lemort V, Quoilin S, Cuevas C, *et al.* Testing and modeling a scroll expander integrated into an Organic Rankine Cycle. *Applied Thermal Engineering* 2009;29:3094–102.
- [16] Oralli E, Md. Ali Tarique, Zamfirescu C, *et al.* A study on scroll compressor conversion into expander for Rankine cycles. *Int J Low-Carbon Technol* 2011;6:200–6.
- [17] Bell I. Theoretical and experimental analysis of liquid flooded compression in scroll compressors. *Ph.D. Dissertation*, Purdue University, 2011.
- [18] Woodland BJ, Braun J, Groll EA, *et al.* Experimental testing of an organic Rankine cycle with Scroll-type expander. In *International Refrigeration and Air Conditioning Conference at Purdue*, 16–19 July 2012, Contribution 2505.
- [19] Engineering Equation Solver, S.A. Klein, 2012.
- [20] Lakew AA, Bolland O. Working fluids for low-temperature heat source. *Appl Thermal Eng* 2010;30:1262–68.
- [21] Chen H, Yogi Goswami D, Stefanakos EK. A review of thermodynamic cycles and working fluids for the conversion of low-grade heat. *Renew Sustain Energy Rev* 2010;14:3059–67.
- [22] Quoilin S, Van Den Broeck M, Declaye S, *et al.* Techno-economic survey of Organic Rankine Cycle (ORC) systems. *Renew Sustain Energy Rev* 2013;22:168–86.
- [23] Quoilin S, Declaye S, Lemort V. Expansion machine and fluid selection for the Organic rankine cycle. In *Proceedings of the 7th International Conference on Heat Transfer, Fluid Mechanics and Thermodynamics*, 2010.
- [24] Lemort V, Declaye S, Quoilin S. Experimental characterization of a hermetic scroll expander for use in a micro-scale Rankine cycle. *Proc Inst Mech Eng A J Power Energy* 2011;226:126–36.
- [25] Kakaç S, Liu H. *Heat Exchangers Selection, Rating and Thermal Design*. University of Miami.
- [26] Calm JM, Hourahan GC. Refrigerant data summary. *Engin Syst* 2001; 18:74–88.
- [27] 3M. <http://solutions.3m.com>.
- [28] Jeffs M, Quintero M, Schmidt U, *et al.* The World Bank OORG—Foam sector. <http://siteresources.worldbank.org/EXTTMP/Resources/JeffsFoamsSector.pdf>.
- [29] Alfa-Biz Limited. Brazed Plate Heat Exchanger. <http://www.alfa-biz.com/Brazed-Plate-Heat-Exchanger.asp>. (1 May 2013, date last accessed).